

Polymorphism and Intersolubility of Some Palmitic, Stearic and Oleic Triglycerides: PPP, PSP and POP

V. Gibon^a, F. Durant^a and Cl. Deroanne^b

^aLaboratoire de Chimie Moléculaire Structurale, Département de Chimie, Facultés Universitaires Notre-Dame de la Paix, 61, rue de Bruxelles, B-5000 NAMUR - Belgium, and ^bChaire de Technologie Agro-Alimentaire, Facultés des Sciences Agronomiques de l'Etat 2, Passage des Déportés, B-5800 GEMBLOUX - Belgium

The polymorphism and intersolubility of a series of palmitic, stearic and oleic triglycerides have been investigated in order to understand the thermal properties of fractions of natural fats. Results are shown for tripalmitin (PPP), 2-stearo-dipalmitin (PSP) and 2-oleo-dipalmitin (POP); these molecules differ essentially in the number of carbons (P→S) and the degree of unsaturation of chains (S→O). The different polymorphic forms have been verified by variable temperature X-ray powder diffraction. The organization of the fatty acid carbon chains in the most stable polymorphic form (β' or β) has been studied by variable temperature NMR spectroscopy by means of the protons relaxation times T_1 , T_2 and $T_{1\rho}$. The construction of binary phase diagrams (PPP-PSP and PPP-POP), from the data obtained by differential scanning calorimetry and X-ray powder diffraction, shows the formation of solid solutions or monotectic interactions, according to the nature and the polymorphic form of the triglycerides. The kinetic of the very important $\beta' \rightarrow \beta$ transition has been analyzed by variable temperature powder X-ray diffraction for PPP, and [PPP-PSP] or [PPP-POP] blends. The molecular interactions occurring between the mixed crystals have been explained by applying the model of Avrami and by an empirical isolation method.

The thermal properties of oil and fat fractions are due mainly to the glycerides and more particularly to the triglycerides. The study of these properties is essential to monitor the technology of natural products (crystallization, fractionation, stabilization of blends . . .).

Triglycerides can crystallize in four polymorphic forms (sub- α , α , β' and β) characterized by a particular carbon chain packing and a specific thermal stability. Precise structural information is available only for the β form (1-5) (single crystal X-ray diffraction); little is known about the β' -form (6). For the other forms, IR spectroscopy (7-17), differential scanning calorimetry (DSC) (18-21), powder X-ray diffraction (22-25), dielectric and microscopic measurements (26-27), dilatometry (28) and NMR spectroscopy (29-34) allow only for hypotheses to be made. Transitions can occur between these forms and are in principal irreversible ($\alpha \rightarrow \beta' \rightarrow \beta$), except for the sub- $\alpha \rightleftharpoons \alpha$ transition, which seems to be reversible (35-36). Because of closely linked structural properties (long chain compounds), triglycerides can produce mixed crystals by intersolubility (37). The most frequent show solid solutions, monotectic interactions, eutectic systems . . . (38-42).

The study of the closely linked polymorphism and intersolubility phenomena allows us to offer some hypotheses on the thermal behavior of the natural fractions of fats (43-44).

MATERIALS AND METHODS

Tripalmitin (PPP) is a Supelco (Bellefonte, Pennsylvania) product, with a GLC purity of ca. 99.5%. 2-Stearo-dipalmitin (PSP) and 2-oleo-dipalmitin (POP) have been synthesized at the Organic Chemistry Laboratory, Facultés des Sciences Agronomiques de l'Etat, Gembloux, Belgium; the GLC purity is ca. 99.5%. The powder X-ray diffraction measurements have been carried out on a PW 1050 Philips diffractometer ($\lambda_{Cu} = 1.54178 \text{ \AA}$) equipped with a temperature control system (Pt probe).

For the study of the $\beta' \rightarrow \beta$ transition, the X-ray detector is set at a diffraction angle characteristic of the β form ($\sim 19.1^\circ [2\theta]$). By following the amplitude of this line as a function of time, we may obtain curves representative of the transition. For the NMR measurements, a Bruker CXP 200 spectrometer ($H_0 = 4.4975$ Teslas) and a Bruker CXP 100 spectrometer ($H_0 = 2.3488$ Teslas) were used.

The DSC measurements were performed on a Setaram DSC 111 calorimeter at a cooling rate of 25 C/min and a heating rate of 5 C/min.

RESULTS AND DISCUSSION

Polymorphism. Powder X-ray diffraction studies. The X-ray powder diffraction lines which are observed around $16\text{-}25^\circ (2\theta)$ for triglycerides are called "short spacings" and are different for each polymorphic form; they correspond to the shortest distances between the fatty acid carbon chains. Moreover, triglycerides may occur as double or triple hydrocarbon chain layers; this can be visualized by the "long spacings" lines occurring between 1 and $15^\circ (2\theta)$. The thus identified polymorphic forms will be named sub- α -2(-3), α -2(-3), β' -2(-3), and β -2(-3), according to the number of different layers of chains (45-46).

Tripalmitin (PPP) is a saturated monoacid triglyceride (16-16-16) which solidifies into α , β' and β forms. The "long spacings" measurements found indicate an "L-2" structure for each polymorphic form.

For 2-stearo-dipalmitin (PSP), a saturated symmetrical mixed triglyceride (16-18-16), the α -2 \rightarrow β'_{1-2} transitions were observed. The two β' forms correspond to recrystallization into a more perfect structure presenting narrower X-ray diffraction lines. The C_{18} stearic chains, which are longer than the palmitic ones, are active at the "terrace" level and prevent the occurrence of any rotations and translations for a $\beta'_{1-2} \rightarrow \beta$ -2 transformation (47).

In 2-oleo-dipalmitin (POP), where the stearic chain is substituted by an oleic chain (with the same number of carbons but one double bond at the 9-10 position), the principal transitions seem to be respectively sub- α -2 \rightleftharpoons α -2 \rightarrow sub- β -2 \rightarrow mixture of forms "L-2" and "L-3" \rightarrow

*To whom correspondence should be addressed.

TABLE 1

Powder X-ray Diffraction Lines (\AA) Associated to the Different Polymorphic forms of POP

	α -2	Sub- β' -2	Mixture of forms L-2 and L-3		Pseudo- β' -2	β -3
short spacings	4.22(vs)	4.39 (s)	5.30 (m)		4.98 (m)	4.62 (vs)
		4.23 (s)	4.78 (s)		4.56 (m)	4.10 (m)
		3.93 (m)	4.50 (m)		4.35 (s)	4.00 (m)
			3.94 (vs)		4.20 (m)	3.86 (m)
			3.63 (s)		4.03 (vs)	3.74 (s)
long spacings	51.9 (n=1)	44.9 (n=1)	49.1 (n=1)	37.6 (n=2)	45.9 (n=1)	62.0 (n=1)
	16.1 (n=3)	15.1 (n=3)	23.9 (n=2)	16.1 (n=4)	21.8 (n=2)	31.1 (n=2)
			14.5 (n=3)		14.7 (n=3)	20.1 (n=3)
					8.5 (n=5)	15.5 (n=4)
	$d_m = 50.1$	$d_m = 45.1$	$d_m = 46.8$	$d_m = 69.8$	$d_m = 43.8$	$d_m = 61.6$
					7.1 (n=6)	10.2 (n=6)

d_m , mean reticular distance; n, order of reflexion; vs, very strong; s, strong; m, medium.

pseudo- β' -2 \rightarrow β -3. The observed "short" and "long spacings" are summarized in Table 1. The "L-2" structure, with saturated and unsaturated chains in the same region, is acceptable only if we consider that "liquid" palmitic chains penetrate inside the region of the mobile oleic chains (sort of liquid crystal structure) (R. Perron, private communication, 1981).

Nuclear magnetic resonance studies. Proton relaxation times T_1 , T_2 and $T_{1\rho}$ have been measured using impulsion sequences: "inversion recovery" for T_1 ; "spin echo" for T_2 , and "spin locking" for $T_{1\rho}$ (48). Cylindrical tubes are filled with triglyceride samples and sealed under vacuum after evacuation of the air. The types of polymorphic forms have been assessed by powder X-ray diffraction and differential scanning calorimetry studies: β -2 for PPP, β' -2 for PSP and β -3 for POP.

T_1 measurements. Andersen and Slichter (49) have studied molecular motions in solid n-alkanes by temperature depending T_1 measurements. In these compounds, the relaxation mechanism is essentially dipolar and the $\lg T_1$ versus temperature variation presents one minimum corresponding to the threefold reorientation of the methyl groups. Tripalmitin and tristearin, in their most stable polymorphic form β -2, present one minimum at 160 K due to the threefold reorientation of the terminal methyl groups (Fig. 1). The methylene groups, being inert at the T_1 minimum temperature, are unable to transfer energy from the spin system to the lattice. Due to rotations at appropriate frequencies, methyl groups are able to transfer this energy, which diffuses into the spin system before being scattered by thermal motions of the lattice; this phenomenon is called spin-diffusion processus (50). The triglycerides T_1 values are three times greater than those of the corresponding alkanes (Table 2). The spin-diffusion processus is less efficient for triglycerides because of the carboxyl groups.

The T_1 thermal variation of 2-stearo-dipalmitin, in its most stable polymorphic form β' -2, is noticeably different from the thermal variation of PPP (Fig. 1). The minimum which is observed at 160 K also corresponds to the threefold reorientation of the methyl groups, but the relaxation processus seems to be less effective than for

TABLE 2

 T_1 Minimal Values (ms) Observed for Some Alkanes (51) and Triglycerides With the Same CH_2/CH_3 Ratio

CH_2/CH_3 Ratio	Alkanes	Triglycerides
14	245	760 (PPP)
16	278	900 (SSS)

TABLE 3

 T_1 Minimal Values (ms) Observed for PPP β -2, PSP β' -2 and POP β -3

Triglycerides	T_1 Minimal Values
PPP β -2	760 (160 K)
PSP β' -2	1130 (160 K)
POP β -3	1220 (160 K) 3070 (275 K)

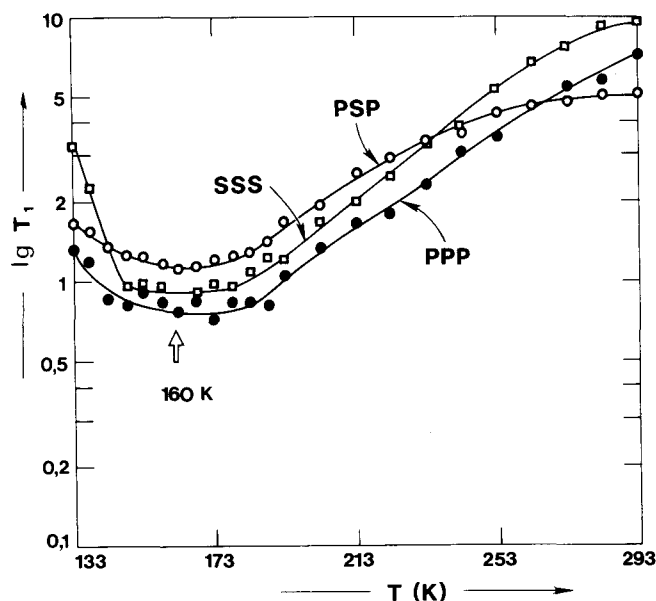


FIG. 1. $\lg T_1$ versus absolute temperature variation observed for SSS β -2 and PSP β' -2 ($H_1 = 30$ Oersted).

POLYMORPHISM OF TRIGLYCERIDES

the monoacid β -2 compound (Table 3); this phenomenon is probably due to the "fishbone" molecular structure advanced for the β' polymorphic form which bends the molecule at the level of the carboxyl groups. The difference between the minimal T_1 values and those at room temperature is greater for PPP β -2 than for PSP β' -2; the methyl region of the β' crystalline structure seems to be less sensitive to thermal perturbations and thus more rigid.

When one stearic chain is substituted by one oleic chain, powder X-ray diffraction indicates a β -3 polymorphic form for 2-oleodipalmitin. The $1g T_1$ thermal variation shows two minima, one at 160 K and the other, not so deep, near 275 K (Fig. 2, Table 3). The first minimum corresponds to the reorientation of the methyl groups (as above), and the second seems to be due to motions of part of the carbon chains. Oleic chains, more mobile than the palmitic ones (000 melting point ca. 6 C and PPP melting point ca. 60 C), are subject to structural reorganization and probably allow the occurrence of this second minimum.

T_2 measurements. The T_2 values observed by Andrew (51) for the n-alkanes present a sudden variation of the profile of the slope of the $1g T_2$ versus the absolute temperature due to some structural transition inside the lattice: orthorhombic symmetry (rotational oscillation) \rightarrow hexagonal symmetry (free rotation). Triglycerides present a constant increase of $1g T_2$ up to the melting point, when they are in their most stable polymorphic form (Fig. 3). We note that two T_2 values appear for POP near 273 K. If we consider the low resolution proton NMR resonance lines of triglycerides, the shape is expected to be structureless according to Chapman et al. (29); however, the small second-moment contribution of the methyl groups and of the CH groups of the glycerol residue may cause the absorption curve to have a weak but narrow component.

This phenomenon is observed for PPP β -2 and PSP β' -2 (Fig. 4). For POP β -3, a more intense narrow line is obtained at room temperature; this could be due not only to the methyl groups' contribution, but also to motions of the oleic chains. Effectively, the spectrum is comparable to that of a fat fraction containing solid and liquid phases, and the contribution of the liquid phase disappears at low temperature. This observation is consistent with the two T_2 values recorded for POP between 273 K and 293 K (Fig. 3).

T_{1Q} measurements. A series of T_{1Q} measurements is shown in Figure 5; they were carried out on PSP β' -2 and POP β -3. These molecules have the same number of carbons in each chain, but, besides the additional presence of a double bond for the oleic fatty acid chain, they also differ in polymorphic form and longitudinal structure. The variation of $1g T_{1Q}$ versus absolute temperature for the alkanes shows one minimum near 90 K corresponding to the threefold reorientation of methyl groups (52). This minimum is not obtained for PSP β' -2 or POP β -3. However, one observes for PSP a different minimum, not so deep, near 253 K, corresponding probably to motions of parts of the chains. For POP, the same minimum is observed at about 243 K, corresponding to motions of the more mobile oleic chains; the progressive $1g T_{1Q}$ reduction at room temperature is probably due to the motions of the palmitic chains.

Intersolubility. [PPP-PSP] and [PPP-POP] temperature-composition binary phase diagrams have been constructed by differential scanning calorimetry and temperature dependent powder X-ray diffraction measurements, in order to understand the thermal behavior and the molecular interactions of simple blends. Those systems have been investigated using a "dynamic processus" of melting, quenching and

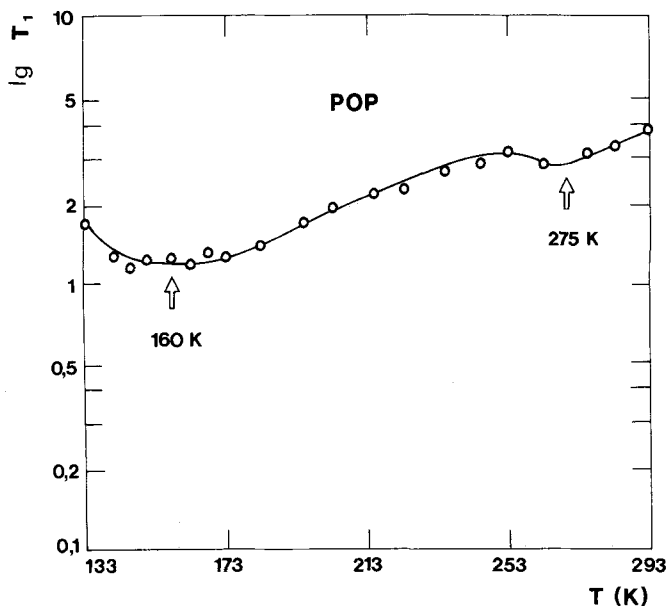


FIG. 2. $1g T_1$ versus absolute temperature variation observed for POP β -3 ($H_1 = 30$ Oerstedts).

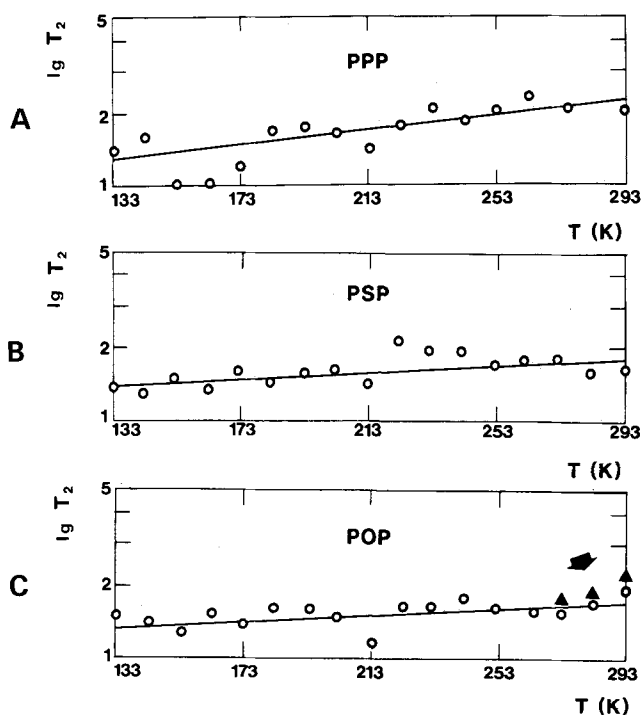


FIG. 3. $1g T_2$ versus absolute temperature variation observed for A, PPP β -2; B, PSP β' -2; C, POP β -3.

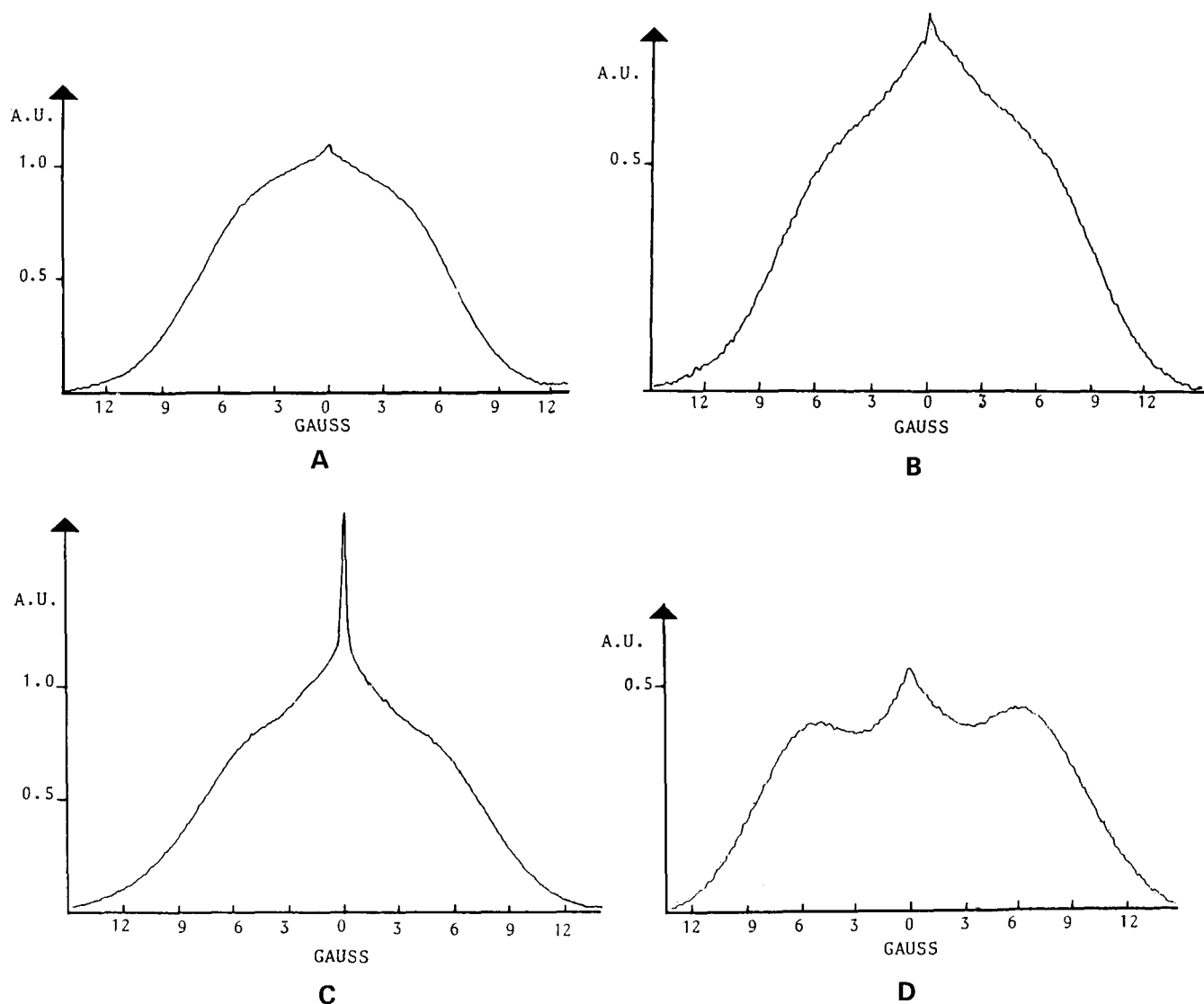


FIG. 4. Proton magnetic resonance absorption lines observed at 298 K for (A) PPP β -2; (B) PSP β' -2; (C), POP β -3 and at 233 K for (D) POP β -3. A.U., arbitrary units.

controlled rate heating. This allows study of the intersolubility for the unstable and stable polymorphic forms. The resulting phase diagrams do not produce real equilibria states but are very interesting from a technological point of view; for this reason, they are not comparable with the earlier papers (39). Each system has been tempered for a few months either at room temperature or 50 C; the resulting phase diagrams show molecular interactions between stable polymorphic forms. These tempered systems do not always crystallize in the thermodynamically most stable phase, but the stabilization is the result of the experimental conditions.

Dynamic study. [PPP-PSP] system (Fig. 6). After melting and quenching, 2-stearo-dipalmitin crystallizes in an α -2 form and changes, when heated at constant rate, into a β' -2 form. This polymorphic form presents, just before the melting, a reduction of the width of the powder X-ray diffraction lines; this transformation is observed by differential scanning calorimetry with the occurrence of an exothermic peak which corresponds to

the recrystallization of the β' -2 into a more perfect β' lattice, β' -2.

In the same conditions, tripalmitin solidifies into an α -2 form and transforms into β' -2 and β -2 phases, after heating at constant rate. Samples with an intermediate composition present solid solutions in the α -2 and β' -2 polymorphic forms. The latter probably corresponds to the PPP β' -2 form. β' -2 form appears very rapidly (a small percentage of PSP); some formation of solid solutions of [PPP-PSP] β' -2 takes place. Only mixed crystals rich in PPP transform into β -2 after eutectic melting; the solubility of PSP in PPP represents about 5%.

[PPP-POP] system (Fig. 7). After melting and quenching, 2-oleo-dipalmitin solidifies into α -2 and transforms, when heated at constant rate, into a sub- β' -2 form, before melting.

Samples with an intermediate composition present α -2 and β' -2 solid solutions; the latter polymorphic form probably corresponds to the PPP β' -2 form. The final melting of the [PPP-POP] system presents a monotectic

POLYMORPHISM OF TRIGLYCERIDES

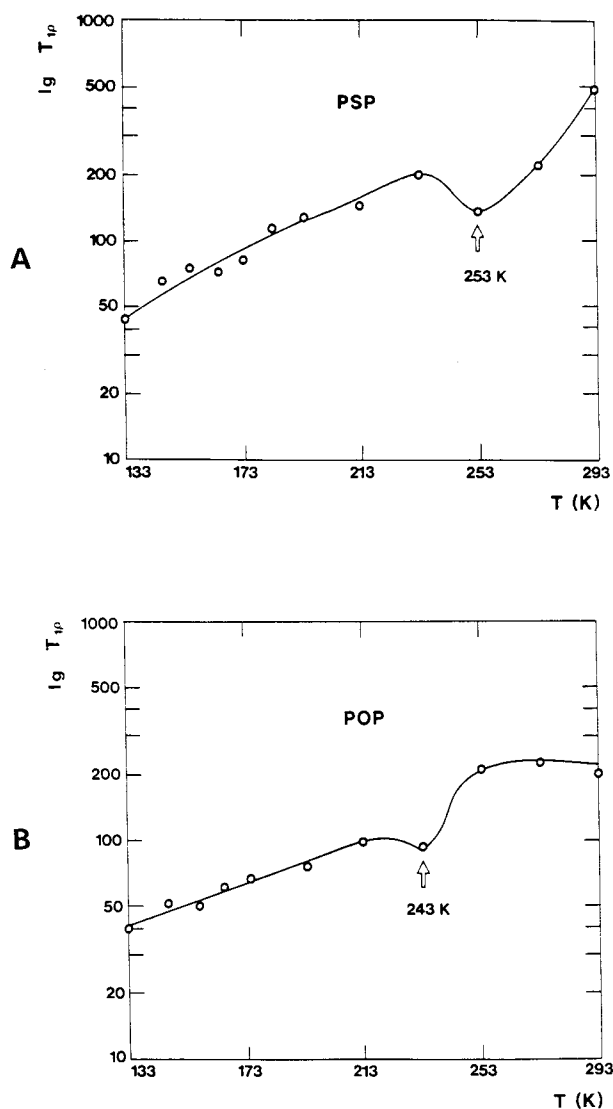


FIG. 5. $\lg T_{10}$ versus absolute temperature variation observed for A, PSP β'_{1-2} ; B, POP $\beta-3$.

interaction in the $\beta-2$ form. The monotectic reaction corresponds to the melting of the $\beta'-2$ solid solution and the recrystallization of a part of the system into $\beta'-2$ [PPP-POP] mixed crystals containing about 15% POP. The $\beta'-2$ mixed crystals transform into $\beta-2$ at the transition temperature. Compounds very rich in POP (more than 95% POP) do not present any β form, the last melting being a $\beta'-2$ form.

The defects created inside the lattice by the longer stearic chains seem less effective than the defects due to the oleic double bond which generates energetically unfavorable voids. One observes rapidly, for the [PPP-POP] system, a separation of the $\beta'-2$ solid solution into $\beta'-2$ mixed crystals containing less than 15% POP. For the [PPP-PSP] system, the perturbation due to the longer stearic hydrocarbon chains takes place at the "terraces" level. The interpenetration of the chains stabilizes the β' form which is observed until the final melting.

Tempered systems. After melting and quenching, the [PPP-POP] system is tempered for a few months at

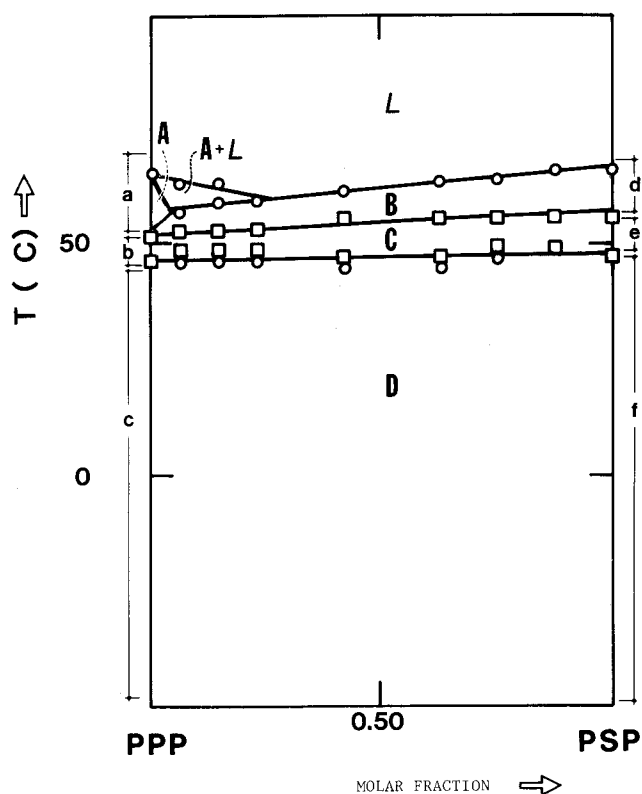


FIG. 6. [PPP-PSP] binary phase diagram constructed after melting, quenching (25 C/min) and heating at constant rate (5 C/min). (O, melting; □, transition). MC, Mixed crystal; SS, solid solution; A, [PPP-PSP] MC $\beta-2$; B, [PPP-PSP] SS β'_{1-2} ; C, [PPP-PSP] SS β'_{2-2} ; D, [PPP-PSP] SS $\alpha-2$, a, PPP $\beta-2$, b, PPP $\beta'-2$, c, PPP $\alpha-2$, d, PSP, β'_{1-2} , e, PSP β'_{2-2} , and f, PSP $\alpha-2$.

room temperature; PPP stabilizes into an $\alpha-2$ and POP into a $\beta-3$ polymorphic form. Due to higher melting points and lower transformation rates, the [PPP-PSP] system has been tempered for a few months at 50 C. At this temperature, PPP stabilizes into a $\beta-2$ and PSP into a β'_{1-2} polymorphic form.

[PPP-PSP] system (Fig. 8). The two pure tempered compounds melt at the same temperature and in the same polymorphic form as the non-tempered ones. At 50 C, the [PPP-PSP] system crystallizes into the extremely unstable β'_{2-2} form which transforms, after tempering, into a β'_{1-2} solid solution. The compounds rich in PPP transform into a $\beta-2$ form with a PSP solubility in the mixed crystals of about 15%. Only one melting is thus observed except for the compounds very rich in PPP.

[PPP-POP] system (Fig. 9). POP transforms itself after tempering from sub- $\beta'-2$ (melting point, 27.5 C) into the most stable $\beta-3$ polymorphic form (melting point, 34.2 C). PPP and mixed crystals rich in PPP stabilize as $\alpha-2$ mixed crystals; $\beta'-2$ crystals transform into $\beta-2$. This allows the existence of $\alpha-2$ crystals, $\alpha-2$ and $\beta-2$ blends and $\beta-2$ crystals in well defined compositions. The sub- $\beta'-2 \rightarrow \beta-3$ POP transformation produces the [PPP-POP] $\beta'-2$ mixed crystals formation; $\beta'-2$ and $\beta-2$ crystals coexist between 45 and 70% POP although $\beta'-2$ mixed crystals and pure $\beta-3$ POP are observed in blends with 70% POP. The monotectic melting corresponds to

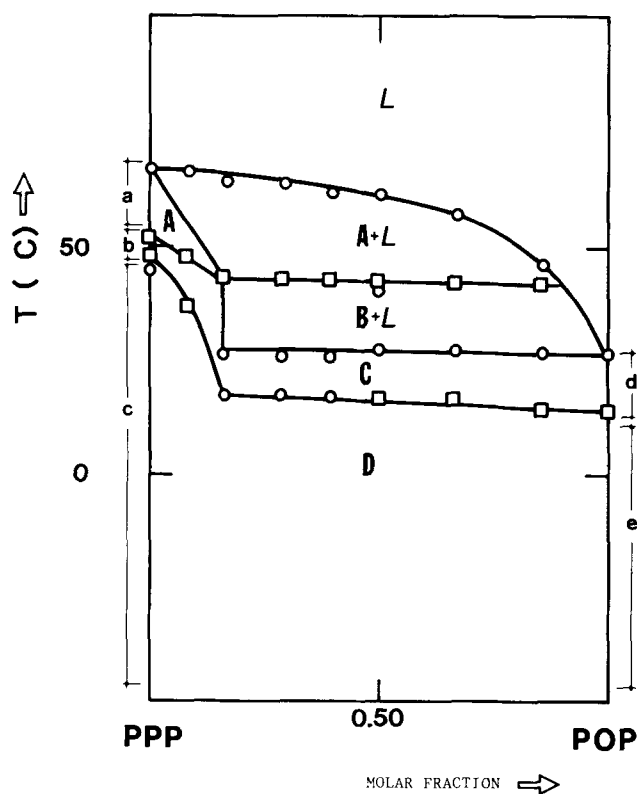


FIG. 7. [PPP-POP] binary phase diagram constructed after melting, quenching (25 C/min) and heating at constant rate (5 C/min). (O, melting; \square , transition). MC, Mixed crystal; SS, solid solution. A, [PPP-POP] MC β -2; B, [PPP-POP] MC β' -2; C, [PPP-POP] SS β' -2; D, [PPP-POP] SS α -2; a, PPP β -2; b, PPP β' -2; c, PPP α -2; d, POP sub- β' -2, and e, POP α -2.

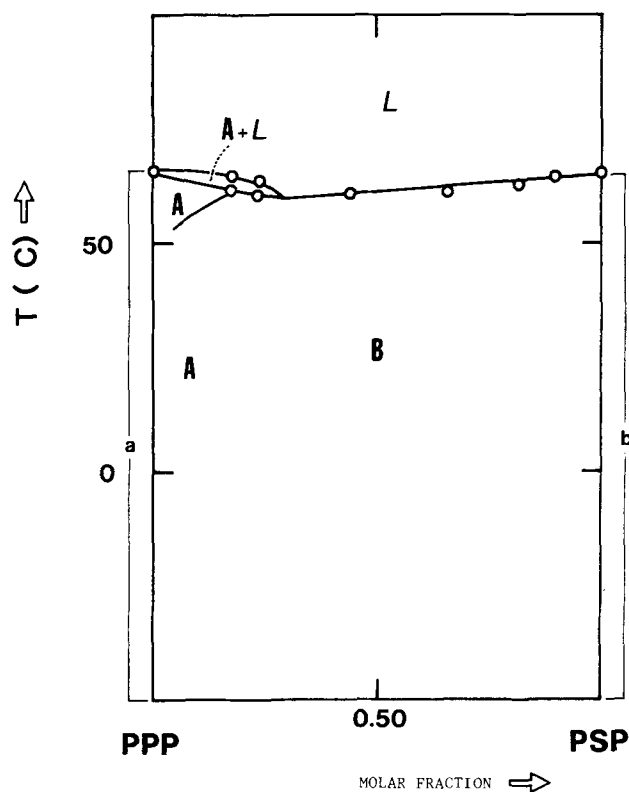


FIG. 8. [PPP-PSP] binary phase diagram constructed after melting, quenching (25 C/min), tempering near the melting point (50 C), quenching (25 C/min) and heating at constant rate (5 C/min); (O, melting; \square , transition). MC, Mixed crystal; SS, solid solution. A, [PPP-PSP] MC β -2; B, [PPP-PSP] SS β' -2; a, PPP β -2, and b, PSP β' -2.

β -3 POP melting and, as in the untempered system, the β' -2 \rightarrow β -2 transition is observed near 39 C. The solubility of POP in PPP is about 70% in β' and 45% in β , and the final melting is of the monotectic type.

The final melting of the [PPP-PSP] tempered system is not changed considerably; except for the blends very rich in PPP where the PSP in PPP solubility is reaching 15%, the phase diagram is not disturbed. The final melting points of the [PPP-POP] tempered system are not strongly altered; the sub- β' -2 \rightarrow β -3 POP transition governs the evolution of the system; a part of the β' -2 solid solution is transformed into a β -2 polymorphic form although the blends rich in POP show a separation into β -3 POP and β' -2 [PPP-POP] mixed crystals. For both systems, an increase in the intersolubility takes place; this relates the β -2 form for [PPP-POP]. The defects seem to be better accepted by the lattice after tempering for a few months.

Kinetics of polymorphism. The $\beta' \rightarrow \beta$ transition has been studied by temperature dependent powder X-ray diffraction for some triglycerides and blends; this transformation is very important due to the crystallization of many triglycerides at room temperature in β' or β . We have shown that the β' -form obtained from the α -form is more unstable than the β' -form directly crystallized from the melt. For pure triglycerides, this phenomenon is due to a better "crystalline perfection" (53) of the β' lattice directly and slowly solidified from

the melt. For blends, the crystalline structure also may differ (mixed crystals, mixture of mixed crystals and pure molecules, etc.) due to a close dependence of the thermal conditioning and crystalline structure. Because of the important undercooling phenomena, we have carried out all our measurements starting from the α obtained β' -form. After melting and quenching (-30 C/min), $\beta' \rightarrow \beta$ kinetic measurements under variable temperatures have been performed on pure PPP, and [PPP-POP] blends, containing a ration of 95/5 (Fig. 10); no liquid phase is present in those mixtures which are essentially mixed crystals. We have chosen to describe the $\beta' \rightarrow \beta$ transition by using the theoretical model of Avrami (54-56). The equation of Avrami, $1 - x = e^{-k t^n}$, with x the β fraction, describes kinetics of the total transformation; n corresponds to the growth of the crystal germs (mono-, bi- or tridimensional) and to the nucleation mode, and k corresponds to the shape of the crystal germs and to the germination and growth rates. Experimental n and k values are obtained by fitting the recorded kinetic curves with the equation of Avrami; the two values allow calculation of activation energy corresponding to the global transformation processus, E_a (57). Note the n value is considered as a characteristic of the curve shape.

It is not possible with this model to separate the nucleation and germination phenomena. In order to isolate the β'/β interfacial growth from the germination

POLYMORPHISM OF TRIGLYCERIDES

TABLE 4

Mean n Values, Global Activation Energy E_a Calculated from the Model of Avrami (cal. mol⁻¹) and Interfacial Growth Activation Energy E_i Calculated from Isolation Measurements (cal. mol⁻¹)

	PPP	[PPP-PSP] 95/5 blend	[PPP-POP] 95/5 blend
n	1.0	1.8	1.3
E_a	70 (4)	84 (3)	67 (3)
E_i	64 (4)	72 (3)	84 (3)

Estimated standard deviation given in parentheses.

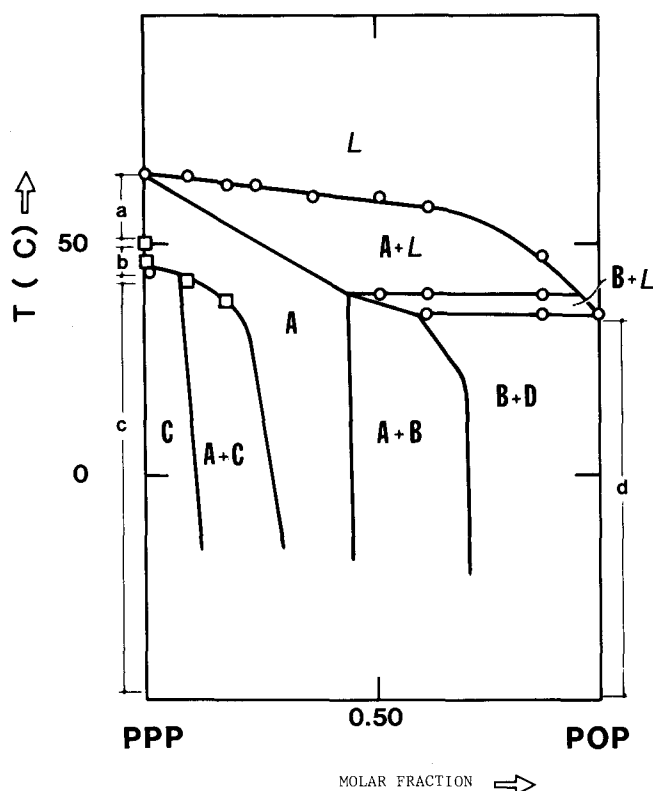


FIG. 9. [PPP-POP] binary phase diagram constructed after melting quenching (25 C/min), tempering at room temperature, quenching (25 C/min) and heating at a constant rate (5 C/min). (O, melting; □, transition). MC, Mixed crystal; SS, solid solution. A, [PPP-POP] MC β -2; B, [PPP-POP] MC β '-2; C, [PPP-POP] MC α -2; D, POP β -3; a, PPP β -2; b, PPP β '-2; c, PPP α -2, and d, D.

process, we have applied an empirical isolation method (58) which consists of melting, quenching and beginning the reaction, interrupting the process by a rapid cooling when the transformation rate is maximal and in continuing it at variable temperatures (Fig. 11). The slope of these curves, just after the temperature change, versus the inverse of the absolute temperature provides an activation energy for the interfacial growth E_i . The E_a and E_i values have been calculated for PPP, [PPP-PSP] and [PPP-POP] blends (Table 4).

Global transformation. The n values obtained for the different blends, after fitting of the transformation curves with the equation of Avrami, have been summarized in Table 4. The calculated values are close to 1 for PPP; they are close to 2 for [PPP-PSP] blends

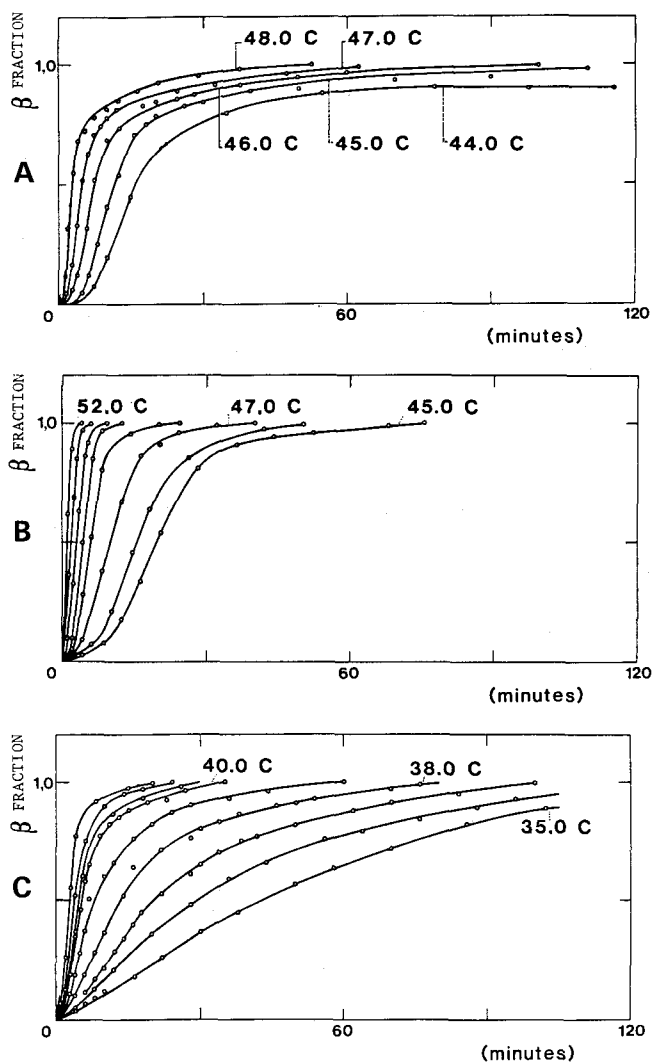


FIG. 10. Variable temperature β' \rightarrow β transitions observed by powder X-ray diffraction for A, PPP; B, [PPP-PSP] 95/5 blend; C, [PPP-POP] 95/5 blend.

and close to 1 for [PPP-POP] blends. An n value of 1 corresponds to the occurrence with a constant probability for space and time of not growing germs (Fig. 12 A); when the n value is close to 2, the nucleation takes place at a constant rate and the germ growth may be monodimensional (Fig. 12 B).

The activation energy E_a values are shown in Table 4. The β' \rightarrow β transition is noticeably hindered for the [PPP-PSP] blend as compared to pure PPP; the important stability of pure PSP in the β' -form conditions this behavior. For the [PPP-POP] blend, a "liquefaction" of the palmitic chains occurs in the region of the more mobile oleic chains (000 melting point ca. 6 C); this furthers the translations and rotations necessary to obtain the β form and accelerates the β' \rightarrow β transition.

Isolation measurements. The activation energy E_i computed from the isolation measurements is gathered in Table 4. [PPP-PSP] and [PPP-POP] values are greater than those observed for PPP. The [PPP-PSP] β'/β interfacial growth rate is reduced due to the occurrence of the stearic chains, slow nucleation and slow interfacial growth. Likewise, the progression of the

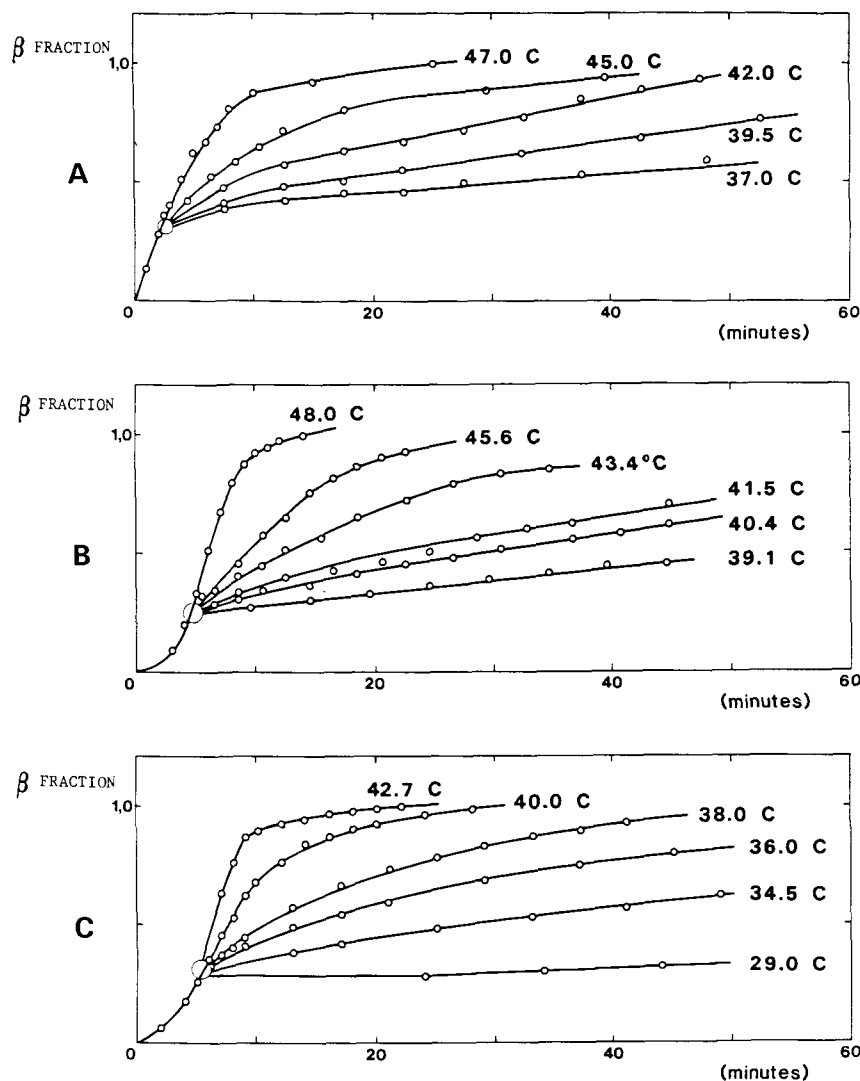


FIG. 11. Isolation process carried out on A, PPP; B, [PPP-PSP] 95/5 blend; C, [PPP-POP] 95/5 blend.

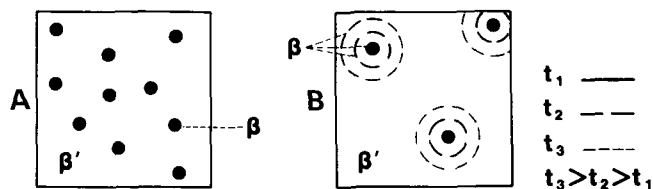


FIG. 12. A, apparition with a constant probability for space and time of germs which do not grow ulteriorly; B, constant rate nucleation and monodimensional germs growth. t , time.

[PPP-POP] β'/β interface is slower than the PPP one. In this case, the lower E_a value is due to a faster nucleation rate in agreement with a slower β'/β interfacial growth.

Although forming very different binary interactions, [PPP-PSP] and [PPP-POP] blends in proportions of 95/5 show quite similar $\beta' \rightarrow \beta$ transition kinetics. We intend to show in another paper how a second stearic or oleic hydrocarbon chain can influence the kinetics of the $\beta' \rightarrow \beta$ transition to a larger extent. The importance of the relative proportions of the triglycerides in a blend also will be discussed.

ACKNOWLEDGMENTS

V. Gibon's work was supported by a grant from the Institut pur l'Encouragement à la Recherche Scientifique dans l'Industrie et l'Agriculture (IRSIA).

REFERENCES

1. Vand, V., and I.P. Bell, *Acta Cryst.* 4:465 (1951).
2. Larsson, K., *Arkiv. Kemi.* 23:1 (1964).
3. Jensen, L.H., and A.J. Mabis, *Acta Cryst.* 21:770 (1966).
4. Doyné, T.H., and J.T. Gordon, *J. Amer. Oil Chem. Soc.* 45:333 (1968).
5. Gibon, V., P. Blanpain, B. Norberg and F. Durant, *Bull. Soc. Chim. Belg.* 93:27 (1984).
6. Hernqvist, L., and K. Larsson, *Fette, Seifen, Anstrichm.* 9:349 (1982).
7. Chapman, D., *J. Chem. Soc.* 55 (1956).
8. Chapman, D., *Ibid.* 2522 (1956).
9. Chapman, D., *Ibid.* 2715 (1957).
10. Corish, P.J., and D. Chapman, *Ibid.* 1747 (1957).
11. Chapman, D., *Ibid.* 1498 (1957).
12. Chapman, D., *Ibid.* 3186 (1958).
13. Chapman, D., *Ibid.* 4860 (1958).
14. Chapman, D., *J. Amer. Oil Chem. Soc.* 37:73 (1960).

15. Chapman, D., *J. Chem. Soc.* 2310 (1962).
16. De Ruig, W.G., Infrared spectra of monoacid triglycerides, Thesis, Utrecht University, 1971.
17. Fringelli, V.P., H.G. Müldner, H.H. Günthard, W. Gasche and W. Leuzinger, *Z. Naturforsch.* 27b:780 (1972).
18. Haighton, A.J., and J.J. Hannewijk, *J. Amer. Oil Chem. Soc.* 35:344 (1958).
19. Perron, R., J. Petit and A. Mathieu, *Chem. Phys. Lipids* 3:11 (1969).
20. Hagemann, J.W., W.H. Tallent and H.E. Kolb, *J. Amer. Oil Chem. Soc.* 49:118 (1972).
21. Deroanne, C., J.M. Marcoen, J.P. Watelet and Severin, M. *J. Thermal Anal.* 11:109 (1977).
22. Clarckson, C.E., and T. Malkin, *J. Chem. Soc.* 666 (1934).
23. Lutton, E.S., *J. Amer. Chem. Soc.* 27:277 (1950).
24. Malkin, T., in *Progress in the Chemistry of Fats and Other Lipids*, Vol. 2, Academic Press Inc., New York, New York, 1954.
25. Larsson, K., *Arkiv. Kemi.* 23:35 (1964).
26. Quimby, O.T., *J. Amer. Chem. Soc.* 72:504 (1950).
27. de Man, J.M., *Food Microstruct.* 1:209 (1982).
28. Hannewijk, J., A.J. Haighton and P.W. Hendricks, in *Analysis and Characterization of Oils, Fats and Fats Products*, Vol. 1, edited by H.A. Bockennoogen, Interscience Pub., London, 1964.
29. Chapman, D., R.S. Richard and R.W. Yorke, *J. Chem. Soc.* 436 (1960).
30. Bailey, A.V., and R.P. Pittman, *J. Amer. Oil Chem. Soc.* 48:775 (1971).
31. Callaghan, P.T., *Chem. Phys. Lipids* 19:56 (1977).
32. Callaghan, P.T., and K.W. Jolley, *J. Chem. Phys.* 67:4773 (1977).
33. Callaghan, P.T., and K.W. Jolley, *Chem. Phys. Lipids* 23:133 (1977).
34. Callaghan, P.T., and K.W. Jolley, *Chem. Phys. Lipids* 27:49 (1980).
35. Chapman, D., *Ibid.* 37:73 (1960).
36. Chapman, D., *Chem. Rev.* 433 (1962).
37. Deroanne, C., M. Severin and B. Wathelet, *Lebensm. Wiss. u.-Technol.* 9:304 (1976).
38. Rossel, J.B., *Adv. Lipid. Res.* 5:353 (1967).
39. Perron, R., J. Petit and A. Mathieu, *Chem. Phys. Lipids* 6:58 (1971).
40. Knoester, M., P. De Bruyne and M. Van den Tempel, *Ibid.* 9:309 (1972).
41. Ollivon, M., and R. Perron, *Chem. Phys. Lipids* 25:395 (1979).
42. Hale, J.E., and F. Schroeder, *Lipids* 6:805 (1981).
43. Deroanne, C., XIII^e Congrès Mondial de la Société Internationale pour l'étude des Corps Gras, Marseille, 1976.
44. Deroanne, C., *Lebensm. Wiss. u. — Technol.* 10:251 (1977).
45. Wille, R.L., and E.S. Lutton, *J. Amer. Oil Chem. Soc.* 43:491 (1966).
46. Deroanne, C., Ph. D. Thesis, University of Gembloux, Belgium, 1978.
47. Lutton, E.S., *J. Amer. Oil Chem. Soc.* 48:245 (1971).
48. Farrar, T.C., and E.D. Becker, in *Pulse and Fourier Transform NMR—Introduction to Theory and Methods*, Academic Press, New York, 1971, pp. 18-34, 87-95.
49. Andersen, J.E., and W.P. Slichter, *J. Phys. Chem.* 69:3099 (1965).
50. McBrierty, V.J., and D.S. Douglass, *Polym. Eng. Sci.* 19:1054 (1979).
51. Andrew, E.R., *J. Chem. Phys.* 18:607 (1950).
52. Douglass, D.C., and E.P. Jones, *J. Chem. Phys.* 45:956 (1966).
53. Dafler, J.R., *J. Amer. Oil Chem. Soc.* 54:249 (1977).
54. Avrami, M., *J. Chem. Phys.* 7:1103 (1939).
55. Avrami, M., *Ibid.* 8:212 (1940).
56. Avrami, M., *Ibid.* 9:177 (1941).
57. Suzuki, A., and R. Tukuda, *Bull. Chem. Soc. Jpn.* 42:1853 (1969).
58. Delmon, B., in *Introduction à la Cinétique Hétérogène*, ed. Technip, 1969. Publ. Institut Francais du Pétrole, pp. 53-105, 244-274, 350-392.

[Received June 13, 1985]

Headpace Volatile Analysis to Evaluate Oxidative and Thermal Stability of Soybean Oil. Effect of Hydrogenation and Additives

J.M. Snyder, E.N. Frankel and K. Warner

Northern Regional Research Center, Agricultural Research Service, U.S. Department of Agriculture, Peoria, IL 61604

Headspace gas chromatographic analysis of heated soybean oil was investigated as a tool to determine what effect hydrogenation and additives have on the formation of total and individual volatile components. Soybean oil was hydrogenated to varying linolenate (Ln) contents with either nickel (Ni) or copper catalysts. Oils were stabilized with citric acid (CA) or a combination of CA with tertiary butyl hydroquinone (TBHQ) and/or methyl silicone (MS). Volatiles were analyzed with a capillary gas chromatograph equipped with a headspace sampler positioned on the injector. Oxidative stability was determined after storage of the oils at 60 C. To study thermal abuse and frying performance of oils, samples were heated for several hours with prolonged bread frying. The deterioration of the oils was accelerated further by static heating in air within the headspace sampler. All hydrogenated oils produced less total volatiles than the unhydrogenated control oil after prolonged heating and bread frying. Static heating at 190 C for one hr showed that the oil hydrogenated with

Ni to 0.4% Ln was the most stable. MS decreased the formation of volatiles in all samples and was particularly effective in stabilizing the hydrogenated oils. However, MS had little effect on volatiles in the oil hydrogenated to 0.4% with Ni. Unique volatile compounds identified included 2,4-heptadienal in non-hydrogenated soybean oil and 2-nonenal in most hydrogenated oils. On heating, the amount of 2-heptanal decreased significantly in the Ni hydrogenated oils compared to the control. Hexanal, on the other hand, decreased in all hydrogenated oils compared to the control.

When fats and oils are heated to frying temperatures, many oxidation reactions occur which produce desirable and undesirable flavors. Polyunsaturated fatty acids are most susceptible to oxidation and promote the formation of volatile compounds in the oils (1-3). Hydrogenation of soybean oil can be effective in producing a more